Synthesis of LaMgAl11O19 powders by reversed microemulsion method

IOP Conf. Series: Materials Science and Engineering **490** (2019) 022048 doi:10.1088/1757-899X/490/2/022048

Synthesis of LaMgAl11O19 powders by reversed microemulsion method

Xiaojiao Zhou, Wei Li*, Song Wang and Qingguo Lei

College of Aerospace Science and Engineering, National University of Defense Technology, Changsha, China

*Corresponding author e-mail: ws0731-nudt@gfkd.mtn

Abstract. The phase behavior of the system employing TritionX-100 as surfactant was investigated with setting different rea-gents as cosurfactant and oil phase at various temperatures and mass ratios of TritionX-100 to cosurfactant. The pseudo-ternary phase diagrams were drawn by using conductivity method. The results indicate that the microemulsion is the most stable and has the best water solubility when the mass ratio of TritionX-100 to hexylalcohol is 1:1. Based on that, LMA powder was synthesized via reversed-microemulsion method using nitrate and ammonia as raw materials. The surface area of LMA powders increases to 53.41m2/g with the increasing water content of the system.

1. Introduction

Lanthanum magnesium hexaaluminate, $LaMgAl_{11}O_{19}$ (LMA) is considered with high potential to be the most promising catalytic materials under high-temperature. LMA is able to maintain high specific surface area because of its layered crystal structure[1.2]. Excellent thermal stability and mechanical performance can be examined under high temperature.The traditional method of synthesizing LMA produces the inhomogeneity of various reactants leading to the impurity phase and low surface area, which seriously affects its appli-cation performance[3.4]. Reverse microemulsion is an efficient method to prepare materials with high specific surface area. In this technique, nanosized micelles dispersed in oil phase are used as microreactor. By carefully adjusting synthesis parameters such as the composition of the reverse microemulsion, water content and aging time, the particle size and specific surface area can be well controlled[5-7]. Therefore, any reverse microemulsion system cannot be used unless its diagram has been studied. In general, the stable reverse microemulsion system with good water-soluble capacity is obtained by drawing the pseudo-ternary phase[8-10]. With $BaAl_{12}O_{19}$, $LaMnAl_{11}O_{19}$ and $CaSnO_3$ being reported to be synthesized by reverse microemulsion, how to synthesize LMA is still a puzzle[11-14].

Herein, We use TritionX-100 as surfactant(S), hexanolnoctanol as cosurfactant (AS), cyclohexane/n-heptane as oil phase(O) and deionized water as water phase(W) to prepare reverse microemulsion. The conductometry was applied to draw the pseudoternary, while synthesis parameters have been systematically studied to obtain a stable microemulsion system. LMA nanoparticles were prepared by reverse micro-emulsion method using metal nitrates as raw materials.

2. Experiment

$Al(NO_3)_3 \cdot 9H_2O$(SCRC), $Mg(NO_3)_2 \cdot 6H_2O$(SCRC) and $La(NO_3)_3 \cdot 6H_2O$ (SCRC) were used as raw materials to fabricate LMA nanoparticles via the reverse microemulsion method. TritionX-100 was

used as the surfactant(S). Hexanol and noctanol(SCRC) were used as cosurfactant. Organic solvents, cyclohexane and n-heptane, were purchased from Sinopharm Chemical Reagent Co.,Ltd. The surfactant, cosurfactant and organic solvent were mixed in a certain proportion. Deionized water was added slowly into the mixture, and the amount of water was recorded at the moment of formation and destruction of the microemulsion. The optimum process parameters were obtained by drawing the pseudo-ternary phase diagram.

Microemulsion A and Microemulsion B were prepared respectively. As for microemulsion A, metal nitrate solution was slowly added into the mixture of surfactant/cosurfactant/oil under magnetic stirring. A homogenous and transparent solution was obtained after continuous stirring. Microemulsion B was made in the same processes except that the metal salts solution was replaced by NH_4OH solutions. The microemulsion B was slowly added into the microemulsion A with vigorous stirring. The mixed system became cloudy and nontransparent. After centrifuging, the precipitation was washed with deionized water and dried in an oven. LMA nanopowder was prepared by roasting the dry precursor.

The crystal phase of the product was measured by X-ray diffraction using a Bruker D8 advance diffractometer. The morphology was investigated using HITACHI scanning electron microscope. Specific surface area, pore volume and aver-age pore diameter were estimated by Quantachrom Quadrasorb SI-3MP surface area analyzer.

3. Results and Discussion

3.1 Drawing the phase diagram of reverse microemulsion

3.1.1The influence of reagent type on microemulsion system

The reaction temperature was stabilized at 30℃. Rea-gents were mixed with a certain ratio to obtain the reverse microemulsion system.Fig.1 shows the phase diagram of the microemulsion system was plotted in the cases of different combinations of reagents. The water-soluble capacity of microemulsion system is stronger with n-heptane substituting cyclohexane as organic solvent. The maximum water content of the system exceeds 50% in the n-heptane/ hexanol. In the cyclohexane/n-hexanol system, the maximum water content of the system is less than 25%. This is due to the difference in compatibility between the isoctyl of TritionX-100 and different organic reagents, so the stability of microemulsion systems are also different. The cosurfactant can change the tension and flexibility of the micelle's interface film and adjust the hydrophilic lipophilic balance(HLB) properties of the surfactant[15]. This regulation is related to the carbon chain length of cosurfactant. The stability of the microemulsion system is reflected by the area bounded by two boundaries in the phase diagram. In Fig 1, there are significant differences in the stability of the microemulsion system when two cosurfactants are used. The stability of the microemulsion system is better when n-hexanol is used. The microemulsion system has the strongest water-soluble capacity and the best stability when n-heptane is selected as oil phase and hexane is selected as cosurfactant.

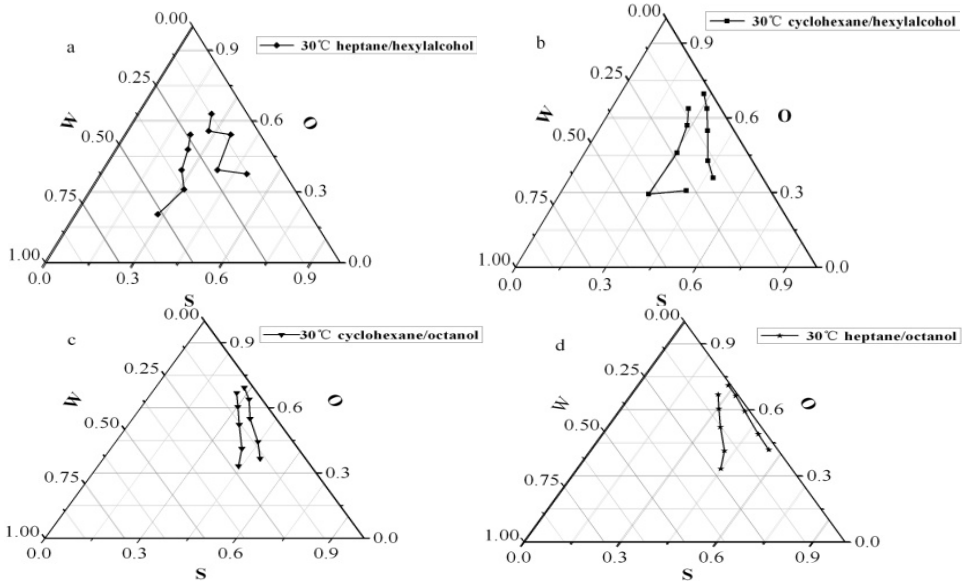

Figure 1. The pseudo-ternary phase diagram of different oil-cosurfactant microemulsion systems: a)heptane/hexylalcohol , b)cyclohexane/hexylalcohol, c)cyclohexane/octanol, d)heptane/octanol.

3.1.2 The influence of reagent proportion on microemulsion system

Fig.2 shows the pseudo-ternary phase diagram of microemulsion system in different situations, when the ratio between S and AS was adjusted to 4:1,2:1,1:1,1:2,1:4 ac-cording to previous research, TritionX-100 was used as surfactant, hexanol and n-heptane were used as cosurfactant and oil phase).With the increase of surfactant dosage, the solubility of the system shows a tendency to increase at first and then decreases. The maximum solubility of the system is 8%,29%, 53%,48% and 26% respectively. The area in the phase diagram varies with the same trend. The presence of hexanol enhances the stability of the microemulsion system. However, when the hexanol content is too high, some hexanol enters into the oil phase, which reduces the strength of the interface film and the stability of the system. The area is the largest when the ratio of S to AS is 1:1, which indicates that the system is the most stable one.

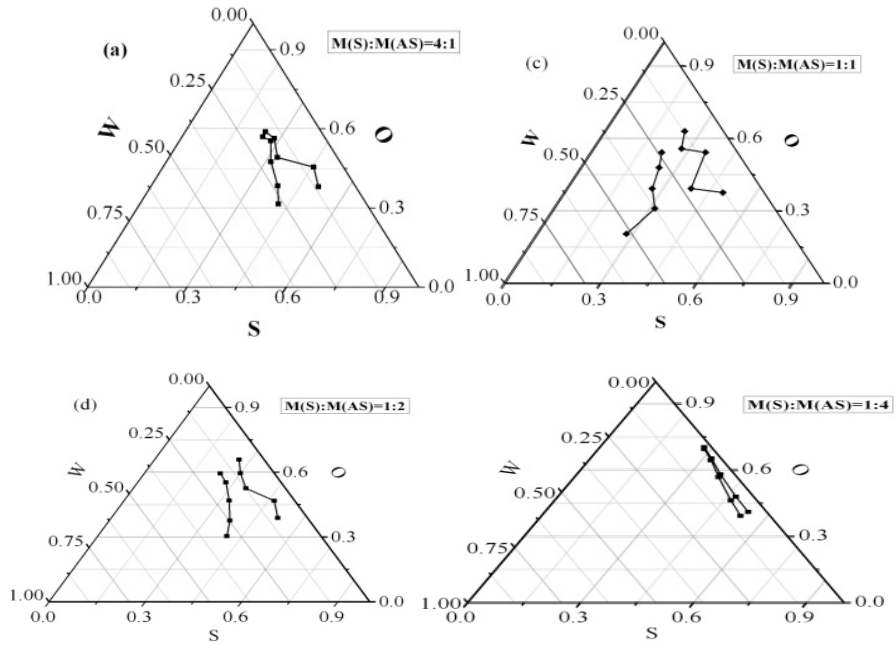

Figure 2. The pseudo-ternary phase diagram of microemulsion systems with variant ratio of S/AS: a)4:1,b)2:1,c)1:1,d)1:2,e)1:4

3.1.3 The influence of temperature on microemulsion system

Fig.3 shows the effect of temperature on the phase diagram of the reverse microemulsion systems. As illustrated in Fig.3, the phase diagrams varies at different temperatures, even in the systems with the same composition and proportion. With the increase of temperature, the maximum soluble water capacity of the system becomes weaker. When the temperature of system is 25℃, the mass fraction of water can be accounted for 60%. When the temperature is 35℃,the proportion fell to only 30%. However, the reverse microemulsion system is more stable at higher temperatures. In the daily production process, the temperature of the system can be adjusted as needed.

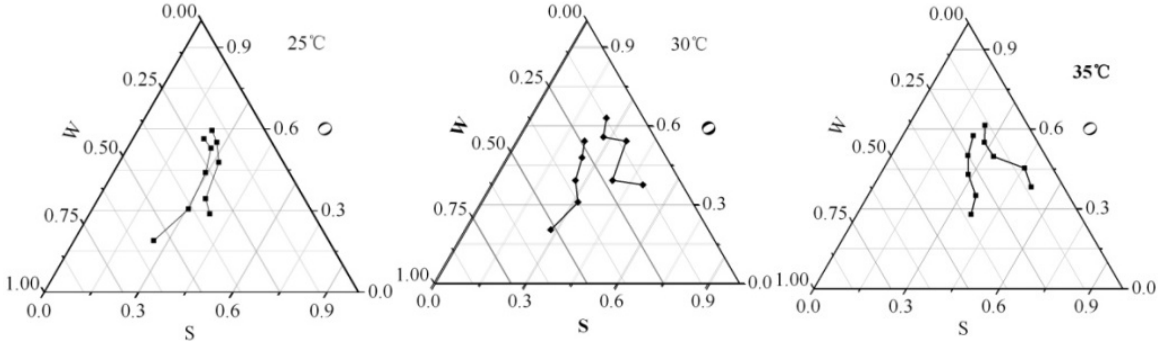

Figure 3. The pseudo-ternary phase diagram of TritionX-100/heptanes/hexylalcohol/water microemulsion systems at 25℃,30℃,35℃

3.2 The synthesis of LMA nanopowder

The LMA was prepared in accordance with the method described in section 2.1, when the water contents of the systems were controlled to be 30%,25%,20%,15, respectively. The XRD diffraction patterns of the prepared samples are presented in Fig.4. The peaks are indexed as 18.92°(101), 32.09°(110),36.19°(101),42.74°(205) respectively. Diffraction patterns corresponding to impurities are found to be absent.

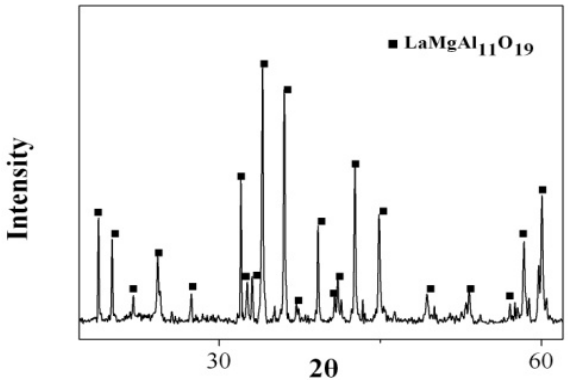

Figure 4. XRD patterns of LMA powders synthesized by microemulsion with different water content

The size of micelle is closely related to the product size when preparing materials by using reverse microemulsion. The size of the product particles can be adjusted by changing the size of the micelles, and the size of the product can also reflect the size of the micelles. It can be seen from Fig.5 that the product presents a lamellar structure formed by the stacking of spherical particles. In the process of high temperature roasting, the precursors undergo sintering to form a larger product, and the larger particles in the picture are the secondary particles formed by sintering. As can be seen from the Fig.5, the particle size is about 15-40nm.The special crystal structure of LMA allows the precursor to change from ball to two-dimensional structure during roasting.

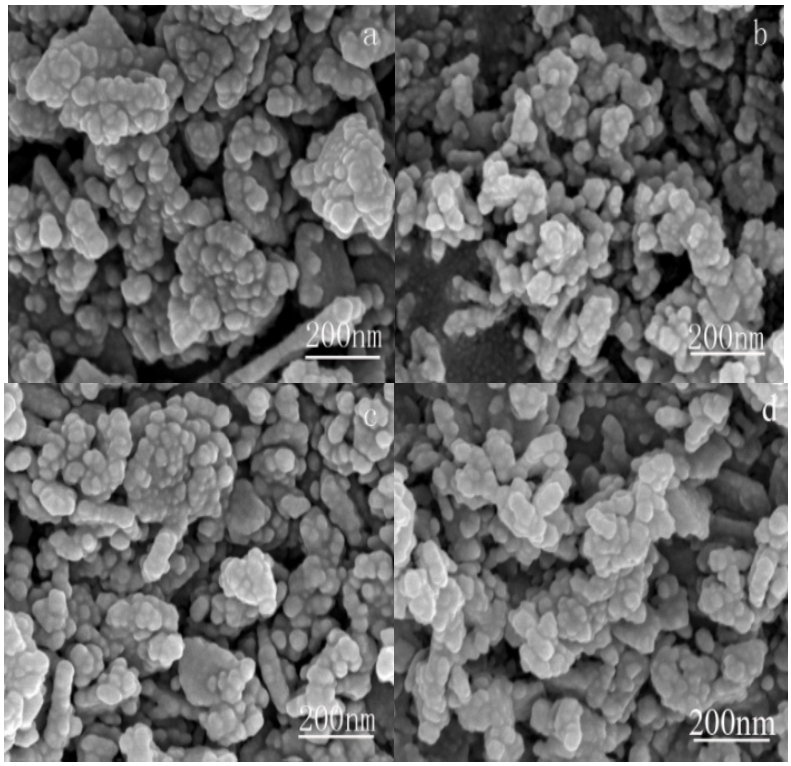

Figure 5. SEM photographs of LMA powders synthesized with different water content: a)30%,b)25%,c)20%,d)15%

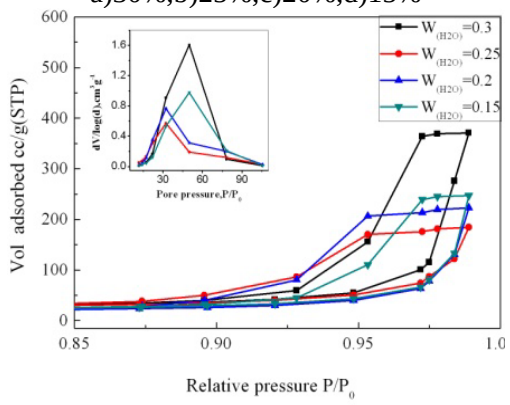

Figure 6. Nitrogen adsorption-desorption isotherms of LMA powder synthesized with different water content. The inset shows the corresponding size distribution curve calculated by the BJH method.

The nitrogen adsorption-desorption isotherms of samples are shown in Fig.6. Isotherms of samples belong to the type-4, and there are hysteresis loops, which indicates that holes of the samples are mainly meroporous. The pore size distribution curve calculated by the BJH method also shows that the pore diameter distribution is concentrated about 30nm-50nm, con-firming the existence of mesoporous.

Table 1. Surface area, pore volume and mean pore diameter of LMA powders synthesized with different water content

Water content	Surface area $m^2 \cdot g^{-1}$	pore volume $cm^3 \cdot g^{-1}$	pore diameter nm
0.30	53.41	0.5742	39.60
0.25	50.58	0.4927	36.55
0.20	46.62	0.1327	11.55
0.15	47.20	0.2036	19.77

Table 1 shows the specific surface area, pore volume and mean pore diameter of several samples. The result indicates that with the increase of the water content of the system, the surface areas of samples become larger, the pore volume and mean pore diameter increase significantly. The specific surface area of the product is 53.41m2/g, when the water content of the system is 30%. According to the percolation theory, the sizes of micelles and precursors increase with the increasing of water content. When the water content of the system is decreased, the size of the precursor particles decrease correspondingly. The particles with smaller size are more likely to be sintered, leading to the reduction of pore volume and pore diameter.

4. Results and Discussion

In summary, LMA nano-powder was synthesized by the reverse microemulsion method. Using tritionX-100 as surfactant, hexanol as cosurfactant, n-heptane as the oil phase, deionized water as the water phase, controlling the ratio of S to AS at 1:1, the maximum dissolved water content is over 50%. After replacing the deionized water with nitrate solution, the amount of dissolved water is more than 30%. The product was well crystallized after a heat treatment at 1200℃.The specific surface area of the product was 53.41m2/g, indicating that the reverse microemulsion method is an effective method for the preparation of high specific surface area materials.

References

[1] Machida M, Eguchi K, Arai H. Journal of Catalyst[J],1987, 103:385
[2] Tian M, Wang X D, Zhang T. Catalysis Science and Technology [J],2016,6:1984
[3] Jiang B, Fang M H, Huang Z H. Material Research Bulletin [J], 2010,45(10):1506
[4] Wu H H, Zhang W Y, Lu S Y et al. Journal of Salt Science and Chemical Industry[J], 2017,46(5):17(in Chinese)
[5] Zarur A J, Mehenti N Z, Heibei A T et al. Langmuir[J], 2000, 16:1968
[6] Zarur A J, Ying J Y et al. Nature[J], 2000,403(7):65
[7] Fan G S, Sun X X, Zhang B B et al. New Chemical Materials[J],2016,5:130
[8] Wang N, Yang L J, Wang X Q et al. Chemical Research and Application [J], 2014,26(8):1200-1209
[9] Yan B, Li H F, Li J. Energy Chemical Industry[J],2016,37(1):60
[10] Peng C Y, Zhou H H, Zeng W et al. Acta Physico-Chimica Sinica[J].2006,22(4):409
[11] Shahdokht S, Hassanzadeh T, Ghashang M. Ceramics International[J],2014,40:9609
[12] Harish K, Renu R et al. International Letters of Chemistry Physics and Astronomy,2013,4:26
[13] Xu J G, Tian Z J, Suo Z H et al. Chinese Journal of Catalysis[J].2005,8(26):665(in Chinese)
[14] W ang L S, Bai S L, Cui M S et al. SCIENTIA SINICA[J]. 2007,37(6):581
[15] Jignasa N, Zagabathuni V P M et al. Industrial and Engineering Chemistry Research[J],2011,50,12311